Theor Chem Acc (2004) 111:25–30
DOI 10.1007/s00214-003-0483-x

Theoretical
Chemistry Accounts

Regular article

Subshell-pair interelectronic angles of atoms

Hisashi Matsuyama, Toshikatsu Koga

Department of Applied Chemistry, Muroran Institute of Technology, Muroran, Hokkaido 050-8585, Japan

Received: 14 April 2003 / Accepted: 17 June 2003 / Published online: 7 October 2003

Abstract. For the 102 atoms from He to Lr in their ground states, the average interelectronic angles $<\theta_{12}>_{nl,n'l'}$ between an electron in a subshell nl and another electron in a subshell $n'l'$ are examined, where n and l are the principal and azimuthal quantum numbers, respectively. Theoretical study clarifies that $<\theta_{12}>_{nl,n'l'}$ are 90° precisely if $|l-l'|$ are even, while they are larger than 90° if $|l-l'|$ are odd. Numerical analysis of 3,275 subshell pairs with odd $|l-l'|$ of the 102 atoms shows that the increases in the total average interelectronic angles $<\theta_{12}>$ from 90° are attributed predominantly to subshell pairs with $n=n'$ and $|l-l'|=1$.

Keywords: Interelectronic angles – Subshell pairs – Atoms

Introduction

In the elucidation of electron–electron interactions of many-electron systems, knowledge of the interelectronic distance, r_{12}, and angle θ_{12} is significant. The interelectronic moments, $<r_{12}^k>$ were reported for the 102 atoms from He (atomic number $Z=2$) to Lr ($Z=103$) in the Hartree–Fock approximation [1, 2] and for the nine atoms from He to Ne based on correlated calculations [3, 4, 5, 6, 7, 8, 9, 10, 11, 12, 13, 14, 15, 16, 17, 18, 19, 20, 21, 22, 23, 24]. On the other hand, little attempt has been made for the evaluation of the interelectronic angle properties. Hartree–Fock expectation values of $\cos\theta_{12}$ were published for the 102 atoms [25], but correlated values were known only for the He and Li atoms [4, 6, 17, 18, 26, 27].

Recently [28], the mathematical structure of the average interelectronic angles, defined by

$$<\theta_{12}> = \frac{2}{N(N-1)}\left\langle \sum_{i=1}^{N-1}\sum_{j=i+1}^{N}\theta_{ij}\right\rangle, \quad (1)$$

was clarified in a general manner and their Hartree–Fock values were reported for the 102 ground-state atoms from He to Lr. In Eq. (1), the angled brackets stand for the expectation value over the N-electron wave function $\Psi(\mathbf{x}_1,\ldots,\mathbf{x}_N)$, with $\mathbf{x}_i=(\mathbf{r}_i,\mathbf{s}_i)$ being the combined position–spin coordinates of the electron i, and θ_{ij} is the angle at the nucleus subtended by the position vectors $\mathbf{r}_i$ and $\mathbf{r}_j$ of the two electrons i and j. It was found [28] that within the Hartree–Fock framework, the average interelectronic angles $<\theta_{12}>$ are always greater than 90°, except for $Z=2$–4 and that the average angle is a maximum (93.17°) at the N atom ($Z=7$). Thus, two electrons have a general tendency to be on opposite sides of the nucleus rather than on the same side.

In the present short paper, we examine the characteristics of the subshell-pair contributions $<\theta_{12}>_{nl,n'l'}$ in the average interelectronic angles $<\theta_{12}>$ within the Hartree–Fock theory of atoms, where n and l are the principal and azimuthal quantum numbers which specify an atomic subshell. Before the interelectronic angles are studied at the correlated level, it is useful to clarify how $<\theta_{12}>$ in atoms are controlled by subshell-pair contributions. The next section presents the mathematical structure of the subshell-pair interelectronic angles $<\theta_{12}>_{nl,n'l'}$. We find that the subshell-pair angles are either 90° ($|l-l'|$ is even) or greater than 90° ($|l-l'|$ is odd). In Sect. 3, numerical analysis of the 102 atoms from He to Lr in their ground states shows that subshell-pair contributions $<\theta_{12}>_{nl,n'l'}$ with $n=n'$ and $|l-l'|=1$ predominantly govern the increase in the total average interelectronic angle from 90°.

Subshell-pair interelectronic angles

According to Ref. [28], we can rewrite Eq. (1) in the form

Correspondence to: T. Koga
e-mail: koga@mmm.muroran-it.ac.jp

$$<\theta_{12}> = \frac{1}{N(N-1)} \sum_{k=0}^{\infty} (2k+1) q_k I_k, \tag{2a}$$

$$q_k = \int \mathrm{d}\mathbf{r}_1 \mathrm{d}\mathbf{r}_2 P_k(\cos\theta_{12}) \Gamma(\mathbf{r}_1, \mathbf{r}_2), \tag{2b}$$

$$I_k = \int_{-1}^{+1} \mathrm{d}x \arccos x \cdot P_k(x), \tag{2c}$$

where $P_k(x)$ is the Legendre polynomial and $\Gamma(\mathbf{r}_1,\mathbf{r}_2)$ is the spinless two-electron density function. The values of the definite integral I_k are [29]

$$I_{2m} = \pi \delta_{m0} \tag{2d}$$

and

$$I_{2m+1} = -\pi \left[\frac{(2m-1)!!}{(2m+2)!!} \right]^2 \tag{2e}$$

for nonnegative integers m, where δ_{ij} is the Kronecker delta. The angles in Eq. (2a) and in this section are measured in radians.

We consider a Hartree–Fock wave function composed of N spin-orbitals $\psi_i(\mathbf{r})\eta_i(s)$. Then, the two-electron density function $\Gamma(\mathbf{r}_1,\mathbf{r}_2)$ is expressed as the sum of spin-orbital-pair contributions $\Gamma_{ij}(\mathbf{r}_1,\mathbf{r}_2)$:

$$\Gamma(\mathbf{r}_1, \mathbf{r}_2) = \frac{1}{2} \sum_{i=1}^{N} \sum_{j=1}^{N} \Gamma_{ij}(\mathbf{r}_1, \mathbf{r}_2), \tag{3a}$$

$$\Gamma_{ij}(\mathbf{r}_1, \mathbf{r}_2) = |\psi_i(\mathbf{r}_1)|^2 |\psi_j(\mathbf{r}_2)|^2 - \delta_{m_{si} m_{sj}} \left[\psi_i^*(\mathbf{r}_1) \psi_j(\mathbf{r}_1) \right] \left[\psi_j^*(\mathbf{r}_2) \psi_i(\mathbf{r}_2) \right], \tag{3b}$$

where m_{si} denotes the spin quantum number of the spin function $\eta_i(s)$. Accordingly, Eq. (2a) is partitioned as

$$<\theta_{12}> = \frac{1}{N(N-1)} \sum_{i=1}^{N} \sum_{j=1}^{N} <\theta_{12}>_{ij}, \tag{4a}$$

$$<\theta_{12}>_{ij} = \sum_{k=0}^{\infty} \frac{2k+1}{2} q_k^{ij} I_k, \tag{4b}$$

$$q_k^{ij} = \int \mathrm{d}\mathbf{r}_1 \mathrm{d}\mathbf{r}_2 P_k(\cos\theta_{12}) \Gamma_{ij}(\mathbf{r}_1, \mathbf{r}_2), \tag{4c}$$

where $<\theta_{12}>_{ii} = 0$ since $\Gamma_{ii}(\mathbf{r}_1,\mathbf{r}_2) = 0$ by the definition in Eq. (3b).

For atomic systems, we assume that a spatial function $\psi_i(\mathbf{r})$ is the product of a radial $R_i(r) = R_{n_i l_i}(r)$ and a spherical harmonic $Y_{l_i m_i}(\theta, \phi)$ function, where m_i stands for the magnetic quantum number and (r,θ,ϕ) is the polar coordinates of the vector $\mathbf{r}$. We first substitute Eq. (3b) into Eq. (4c) and expand the Legendre polynomial $P_k(\cos\theta_{12})$ in terms of spherical harmonics. On integrating the resultant expression for q_k^{ij} with respect to the angular variables, we then find that Eq. (4b) is given by

$$<\theta_{12}>_{ij} = \frac{\pi}{2} - \delta_{m_{si} m_{sj}} |S(i,j)|^2 \sum_{k=|l_i - l_j|}^{l_i + l_j} \frac{2k+1}{2} b^k(l_i m_i, l_j m_j) I_k, \tag{5a}$$

$$S(i,j) = \int_0^{\infty} \mathrm{d}r r^2 R_i^*(r) R_j(r) = S^*(j,i), \tag{5b}$$

in which $b^k(lm,l'm')$ is the Condon–Shortley parameter [30, 31] and the summation index k runs over every other integer. Note that owing to the property of I_k, the summation vanishes for even values of $l_i + l_j$. From Eq. (5a), we immediately obtain

$$<\theta_{12}>_{ij} = \frac{\pi}{2} \tag{6a}$$

if $m_{si} \neq m_{sj}$ or $|l - l'|$ is even since the second term vanishes, and

$$<\theta_{12}>_{ij} > \frac{\pi}{2} \tag{6b}$$

if $m_{si} = m_{sj}$ and $|l - l'|$ is odd since $b^k(lm,l'm')$ is positive and I_k is negative. Namely, the exchange effect between two electrons with parallel spins and different space reflection symmetries works to increase the interelectronic angle from $\pi/2$.

The subshell-pair interelectronic angle $<\theta_{12}>_{nl,n'l'}$ is defined by

$$<\theta_{12}>_{nl,n'l'} = \frac{1}{N_{nl,n'l'}} \sum_{i=1}^{N} \sum_{j=1}^{N} \delta_{n n_i} \delta_{l l_i} \delta_{n' n_j} \delta_{l' l_j} <\theta_{12}>_{ij}, \tag{7}$$

where $N_{nl,n'l'}$ is the number of electron pairs for the electrons in two different subshells nl and $n'l'$. If the two electrons are in the same subshell, $N_{nl,n'l'}$ is twice the number of possible electron pairs. When we consider the 102 atoms from He to Lr in their experimental ground states, no subshells with g or higher azimuthal quantum numbers appear. Thus, the $<\theta_{12}>_{nl,n'l'}$ of *ss*, *sd*, *pp*, *pf*, *dd*, and *ff* subshell pairs are $\pi/2$ precisely, whereas those of *sp*, *sf*, *pd*, and *df* subshell pairs are larger than $\pi/2$. In the former case, the position vectors $\mathbf{r}_i$ and $\mathbf{r}_j$ of the two electrons are perpendicular on average, and in the latter case, two electrons have more probability to be on opposite sides of the nucleus than on the same side.

Numerical results and discussion

The experimental ground electronic configurations and *LS* terms [32] were considered for all the 102 atoms from

He to Lr. For these states, the radial functions $R_i(r)$ were generated by the numerical Hartree–Fock method based on a modified version of the MCHF72 program [33]. The b^k values were taken from Refs. [30, 31]. In the subsequent discussion, numerical values of the interelectronic angles are given in degrees.

As an example, we consider the Rn atom ($Z=86$) with the fully occupied 1*s*–6*s*, 2*p*–6*p*, 3*d*–5*d*, and 4*f* subshells. Since the Rn atom has 15 subshells, there are 120 subshell pairs arising from combinations of two subshells nl and $n'l'$. Among the 120 pairs, 66 subshell pairs have even $|l-l'|$, while 54 subshell pairs have odd $|l-l'|$. As already mentioned, $<\theta_{12}>_{nl,n'l'}$ of the 66 subshell pairs are 90°. The remaining 54 subshell-pair angles are classified in Table 1 into six groups according to the values of $|n-n'|$ for our later convenience. In the table, we find two features in the $<\theta_{12}>_{nl,n'l'}$ values. For the 44 subshell pairs with $|n-n'|\geq 1$, the average interelectronic angles are close to 90°, although there are a few exceptions. On the other hand, $<\theta_{12}>_{nl,n'l'}$ of the nine subshell pairs with $n=n'$ (except for 4*s*4*f*) are considerably larger than 90° and are strongly dependent on the combination of l and l'. When $n=n'=4$, for example, the increases of the *sp*, *pd*, *df*, and *sf* angles from 90° are 11.02, 4.46, 2.31, and 0.42°, respectively. The ratios of these values are 26.2:10.6:5.5:1. On the basis of Eqs. (5a) and (7), the difference of the average interelectronic angles from 90° for the closed N ($n=4$) shell is explicitly written in degrees as

$$<\theta_{12}>_{4l4l'} -90 = C_{ll'}|S(4l,4l')|^2, \quad (8)$$

where the coefficients $C_{ll'}$ are $C_{sp}=45/4$, $C_{pd}=315/64$, $C_{df}=405/128$, and $C_{sf}=45/64$. The ratios of these values are 16:7:4.5:1, and the result is not far from the ratios observed in the calculated angles. Similar trends are observed for the other n values. Thus, the increases in the subshell-pair interelectronic angles in a shell are found to depend mainly on b^k and I_k rather than on $|S(nl,nl')|^2$. It is also suggested that the subshell pairs with $n=n'$ and $|l-l'|=1$ are important for the increase in the interelectronic angle.

Table 1 also includes electron repulsion energies $<1/r_{12}>_{nl,n'l'}$ [34] between an electron in a subshell nl and another electron in a subshell $n'l'$ based on numerical Hartree–Fock calculations. The 54 subshell pairs in Table 1 are classified into 20 groups according to the combination of n and n'. We have examined the correlation between $<\theta_{12}>_{nl,n'l'}$ and $<1/r_{12}>_{nl,n'l'}$ of ten groups which have three or more subshell pairs. We find that four groups, 2*l*5*l'*, 4*l*4*l'*, 3*l*5*l'*, and 2*l*3*l'* have good linear correlations, whose correlation coefficients (CCs) are −0.9997, −0.9961, −0.9721, and 1.000, respectively. This means that when the average interelectronic angle increases within a group, $<1/r_{12}>_{nl,n'l'}$ decreases for the first three groups, while it increases for the fourth group. The absolute values of the CCs for the other six groups distribute between 0.1044 and 0.6947. At present, we do not have any good physical

Table 1. The average interelectronic angles $<\theta_{12}>_{nl,n'l'}$ and electron repulsion energies $<1/r_{12}>_{nl,n'l'}$ of 54 subshell pairs with odd $|l-l'|$ for the Rn atom

$\|n-n'\|$	Subshell pair	$<\theta_{12}>_{nl,n'l'}$	$<1/r_{12}>_{nl,n'l'}$	$\|n-n'\|$	Subshell pair	$<\theta_{12}>_{nl,n'l'}$	$<1/r_{12}>_{nl,n'l'}$
0	2*s*2*p*	98.735	11.9234	2	1*s*3*p*	90.424	7.6076
	3*s*3*p*	100.444	4.4470		2*s*4*p*	90.066	3.1173
	3*p*3*d*	93.263	5.1612		2*s*4*f*	90.011	2.9905
	4*s*4*p*	101.019	1.9921		2*p*4*s*	90.006	3.1247
	4*s*4*f*	90.423	2.1951		2*p*4*d*	90.262	3.1808
	4*p*4*d*	94.456	2.1064		3*s*5*p*	90.008	1.3155
	4*d*4*f*	92.314	2.1668		3*p*5*s*	90.001	1.3830
	5*s*5*p*	101.102	0.8950		3*p*5*d*	90.027	1.1580
	5*p*5*d*	94.580	0.8525		3*d*5*p*	90.001	1.3334
	6*s*6*p*	100.555	0.3394		4*s*6*p*	90.000	0.4709
1	1*s*2*p*	92.364	19.0519		4*p*6*s*	90.000	0.5483
	2*s*3*p*	90.306	6.4747		4*d*6*p*	90.000	0.4712
	2*p*3*s*	90.028	6.2982		4*f*6*s*	90.000	0.5494
	2*p*3*d*	91.636	7.3381	3	1*s*4*p*	90.100	3.3867
	3*s*4*p*	90.037	2.7634		1*s*4*f*	90.000	2.9970
	3*s*4*f*	90.248	2.8341		2*s*5*p*	90.013	1.3830
	3*p*4*s*	90.005	2.7779		2*p*5*s*	90.001	1.4553
	3*p*4*d*	90.184	2.8195		2*p*5*d*	90.037	1.2108
	3*d*4*p*	90.003	2.8592		3*s*6*p*	90.001	0.4814
	3*d*4*f*	90.817	2.8825		3*p*6*s*	90.000	0.5638
	4*s*5*p*	90.001	1.2113		3*d*6*p*	90.000	0.4833
	4*p*5*s*	90.004	1.2650	4	1*s*5*p*	90.020	1.4357
	4*p*5*d*	90.000	1.0750		2*s*6*p*	90.001	0.4884
	4*d*5*p*	90.009	1.2148		2*p*6*s*	90.000	0.5735
	4*f*5*s*	90.019	1.2734	5	1*s*6*p*	90.002	0.4940
	4*f*5*d*	90.025	1.0762				
	5*s*6*p*	90.031	0.4484				
	5*p*6*s*	90.052	0.5135				
	5*d*6*p*	90.150	0.4399				

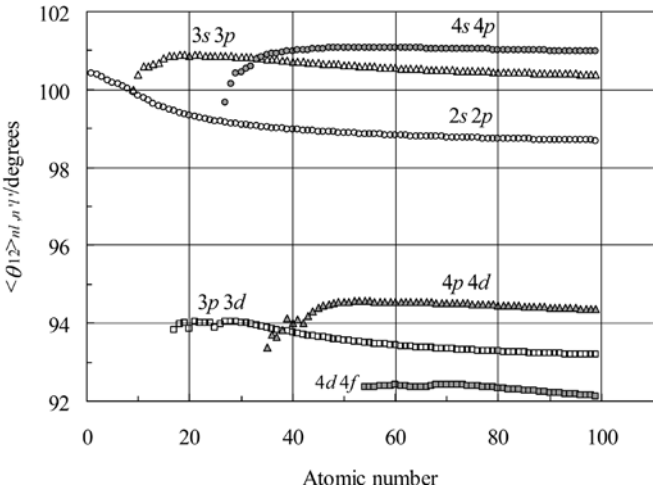

Fig. 1. The Z dependence of some representative subshell-pair interelectronic angles $<\theta_{12}>_{nl,n'l'}$ with $n=n'$ and $|l-l'|=1$

interpretation for the correlation between $<\theta_{12}>_{nl,n'l'}$ and $<1/r_{12}>_{nl,n'l'}$, which is good sometimes but poor at other times.

In the 102 atoms, there are 188 different kinds of subshell pairs, consisting of 101 kinds with even $|l-l'|$ and 87 kinds with odd $|l-l'|$. The total number of the 87 kinds of subshell pairs with odd $|l-l'|$ is 3,275 for the 102 atoms. The Z dependence of several representative subshell-pair angles $<\theta_{12}>_{nl,n'l'}$ with $n=n'$ and $|l-l'|=1$ is shown in Fig. 1. Except for some atoms with smaller Z, the subshell-pair interelectronic angles remain almost constant. We calculated the mean value of $<\theta_{12}>_{nl,n'l'}$ for each of the 87 subshell pairs with odd $|l-l'|$ and summarized the results in Table 2 in the increasing order of $|n-n'|$. The mean angles are largest when $n=n'$ and decrease towards 90° as $|n-n'|$ increases. The maximum angles are 100.96° ($4s4p$ pair) when $n=n'$, 92.05° ($1s2p$ pair) when $|n-n'|=1$, and 90.33° ($1s3p$

Table 2. The mean values of $<\theta_{12}>_{nl,n'l'}$ for 87 kinds of subshell pairs with odd $|l-l'|$ of the 102 atoms from He to Lr in their ground states

$\|n-n'\|$	Subshell pair	No. of pairs	Mean value	$\|n-n'\|$	Subshell pair	No. of pairs	Mean value
0	2*s*2*p*	99	99.069	2	2*p*4*d*	65	90.204
	3*s*3*p*	91	100.604		3*s*5*p*	55	90.005
	3*p*3*d*	83	93.540		3*s*5*f*	13	90.023
	4*s*4*p*	73	100.959		3*p*5*s*	66	90.001
	4*s*4*f*	46	90.418		3*p*5*d*	36	90.025
	4*p*4*d*	65	94.399		3*d*5*p*	55	90.000
	4*d*4*f*	46	92.319		3*d*5*f*	13	90.083
	5*s*5*p*	55	100.922		4*s*6*p*	23	90.000
	5*s*5*f*	13	90.430		4*p*6*s*	49	90.000
	5*p*5*d*	36	94.343		4*p*6*d*	6	90.000
	5*d*5*f*	13	92.526		4*d*6*p*	23	90.000
	6*s*6*p*	23	100.673		4*f*6*s*	46	90.000
	6*p*6*d*	6	93.664		4*f*6*d*	6	90.000
	7*s*7*p*	1	99.972		5*s*7*p*	1	90.001
1	1*s*2*p*	99	92.051		5*p*7*s*	17	90.002
	2*s*3*p*	91	90.208		5*d*7*p*	1	90.002
	2*p*3*s*	93	90.018		5*f*7*s*	13	90.000
	2*p*3*d*	83	91.297	3	1*s*4*p*	73	90.074
	3*s*4*p*	73	90.022		1*s*4*f*	46	90.000
	3*s*4*f*	46	90.209		2*s*5*p*	55	90.010
	3*p*4*s*	85	90.011		2*s*5*f*	13	90.002
	3*p*4*d*	65	90.121		2*p*5*s*	66	90.001
	3*d*4*p*	73	90.009		2*p*5*d*	36	90.035
	3*d*4*f*	46	90.697		3*s*6*p*	23	90.001
	4*s*5*p*	55	90.007		3*p*6*s*	49	90.000
	4*s*5*f*	13	90.005		3*p*6*d*	6	90.003
	4*p*5*s*	66	90.026		3*d*6*p*	23	90.000
	4*p*5*d*	36	90.004		4*s*7*p*	1	90.000
	4*d*5*p*	55	90.035		4*p*7*s*	17	90.000
	4*d*5*f*	13	90.013		4*d*7*p*	1	90.000
	4*f*5*s*	46	90.064		4*f*7*s*	17	90.000
	4*f*5*d*	35	90.099	4	1*s*5*p*	55	90.015
	5*s*6*p*	23	90.026		1*s*5*f*	13	90.000
	5*p*6*s*	49	90.082		2*s*6*p*	23	90.002
	5*p*6*d*	6	90.037		2*p*6*s*	49	90.000
	5*d*6*p*	23	90.116		2*p*6*d*	6	90.004
	5*f*6*s*	13	90.237		3*s*7*p*	1	90.000
	5*f*6*d*	4	92.014		3*p*7*s*	17	90.000
	6*s*7*p*	1	90.062		3*d*7*p*	1	90.000
	6*p*7*s*	17	90.143	5	1*s*6*p*	23	90.003
2	1*s*3*p*	91	90.325		2*s*7*p*	1	90.000
	2*s*4*p*	73	90.047		2*p*7*s*	17	90.000
	2*s*4*f*	46	90.009	6	1*s*7*p*	1	90.000
	2*p*4*s*	85	90.004				

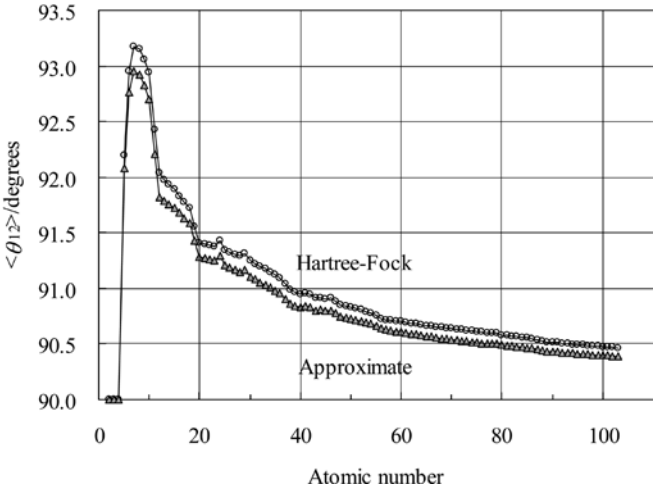

Fig. 2. The Hartree–Fock interelectronic angles $<\theta_{12}>$ and their approximations $<\theta_{12}>_{ap}$ for the 102 ground-state atoms

pair) when $|n-n'| \geq 2$, respectively. Two electrons in the same shell have analogous radial distributions and they try to avoid each other by increasing the interelectronic angle.

For the 14 subshell pairs with $n=n'$, the mean values of the interelectronic angles in Table 2 are largely dependent on the combination of l and l' as was the case of the Rn atom in Table 1. The *sp*, *pd*, *df*, and *sf* pairs have mean values of about 100, 94, 92, and 90°, respectively. Numerical analysis of 3,275 pairs with odd $|l-l'|$ concludes that the increases in the total average interelectronic angles from 90° are mainly attributed to the *sp*, *pd*, and *df* subshell-pair contributions with $|l-l'|=1$. More specifically, we can choose 12 subshell pairs, six *nsnp* ($n=2$–7), four *npnd* ($n=3$–6), and two *ndnf* ($n=4$, 5), as major subshell pairs which increase the average interelectronic angles of atoms from 90°. We then introduce an approximate average interelectronic angle $<\theta_{12}>_{ap}$ given in degrees by

$$<\theta_{12}>_{ap} = \frac{2}{N(N-1)} \times \left\{ \sum_{n=2}^{7} N_{nsnp} <\theta_{12}>_{nsnp} + \sum_{n=3}^{6} N_{npnd} <\theta_{12}>_{npnd} + \sum_{n=4}^{5} N_{ndnf} <\theta_{12}>_{ndnf} + N_{\text{others}} \times 90 \right\}, \quad (9)$$

where N_{others} is the number of possible electron pairs in the other subshell pairs except for the 12 pairs mentioned earlier.

The approximation $<\theta_{12}>_{ap}$ is compared to the Hartree–Fock $<\theta_{12}>$ for the 102 atoms in Fig. 2. For the first three atoms with $Z=2$–4, $<\theta_{12}>_{ap}$ coincides with $<\theta_{12}>$. For $Z>5$, $<\theta_{12}>_{ap}$ is always smaller than $<\theta_{12}>$, but the mean relative error is only 0.12% with the maximum 0.25% at the Ne atom. As depicted in Fig. 2, the Hartree–Fock interelectronic angles $<\theta_{12}>$ of the atoms in their ground states are known [28] to increase from $Z=2$ to $Z=6$, have a maximum at $Z=7$, and decrease gradually from $Z=8$ to $Z=103$. Equation (9) clarifies the observed Z dependence of $<\theta_{12}>$. In particular, the maximum (93.17°) at $Z=7$ is explained by the relative significance of three $2s2p$ electron pairs with parallel spins among the total 21 electron pairs.

Summary

The average interelectronic angles $<\theta_{12}>_{nl,n'l'}$ between an electron in a subshell nl and another electron in a subshell $n'l'$ have been studied for the 102 atoms from He to Lr in their ground states. $<\theta_{12}>_{nl,n'l'}$ are 90° precisely if $|l-l'|$ is even, while they are larger than 90° if $|l-l'|$ is odd. The increases in the total average interelectronic angles $<\theta_{12}>$ from 90° are mainly due to the *sp*, *pd*, and *df* subshell pairs in the same shell.

Acknowledgements. We thank D. Yokota for his assistance in the compilation of data. This work was supported in part by a Grant-in-Aid for Scientific Research from the Ministry of Education of Japan.

References

1. Koga T, Matsuyama H (1997) J Chem Phys 107:8510
2. Koga T, Matsuyama H (1999) J Chem Phys 111:9191
3. Pekeris CL (1959) Phys Rev 115: 1216
4. Thakkar AJ, Smith VH Jr (1977) Phys Rev A 15:1
5. Banyard KE, Mobbs RJ (1981) J Chem Phys 75:3433
6. Regier PE, Thakkar AJ (1985) J Phys B 18:3061
7. King FW (1989) Phys Rev A 40:1735
8. King FW, Bergsbaken MP (1990) J Chem Phys 93:2570
9. Wang J, Tripathi AN, Smith VH Jr (1992) J Chem Phys 97:9188
10. Koga T, Kasai Y, Thakkar AJ (1993) Int J Quantum Chem 46:689
11. Dressel PR, King FW (1994) J Chem Phys 100:7515
12. Yan Z-C, Drake GWF (1995) Phys Rev A 52:3711
13. Komasa J, Cencek W, Rychlewski J (1995) Phys Rev A 52:4500
14. Arias de Saavedra F, Porras I, Buendia E, Galvez FJ (1995) J Phys B 28:3123
15. King FW (1995) J Chem Phys 102:8053
16. Drake GWF (1996) In: Drake GWF (ed) Atomic, molecular, and optical physics handbook. AIP, New York, p 154
17. Montgomery HE Jr (1998) Chem Phys Lett 294:468
18. Frolov AM (1998) Phys Rev A 57:2436
19. Sarsa A, Galvez FJ, Buendia E (1998) J Chem Phys 109:7075
20. Galvez FJ, Buendia E, Sarsa A (1999) J Chem Phys 111:10903
21. Koga T (2001) Chem Phys Lett 350:135
22. Galvez FJ, Buendia E, Sarsa A (2001) J Chem Phys 115:1166
23. Koga T (2002) Theor Chem Acc 107:246
24. Koga T (2002) J Chem Phys 116:6614
25. Koga T (2002) Chem Phys Lett 363:598
26. Banyard KE, Baker CC (1969) J Chem Phys 51:2680
27. Banyard KE, Al-Bayati KH (1986) J Phys B 19:2211
28. Koga T (2002) J Chem Phys 117: 10493
29. Gradshteyn IS, Ryzhik IM (1980) Table of integrals, series, and products. Academic, San Diego, p 825

30. Condon EU, Shortley GH (1970) The theory of atomic spectra. Cambridge University Press, London
31. Condon EU, Odabasi H (1980) Atomic structure. Cambridge University Press, Cambridge
32. Avery J (2003) In: Wilson S (ed) Handbook of molecular physics and quantum chemistry, vol 1. Wiley, Chichester, p 236
33. Froese Fischer C (1972) Comput Phys Commun 4:107
34. Koga T, Matsuyama H (1998) J Phys B 31:5105